Investigating the superconducting properties and surface morphology of sputtered Nb films on Cu due to laser treatment

Daniel Andrew Turner, O. B. Malyshev, G. Burt, E. Seiler, R. Ries, A. Medvids, P. Onufrijevs, R. Valizadeh, A. Sublet, C. Pira, E. Chyhyrynets, M. Vogel, S. Leith, T. Junginger

***Abstract*—Bulk niobium is currently the material of choice for superconducting radio frequency (SRF) cavities and is a well matured process. However, it is possible that SRF cavities could be further improved beyond bulk Nb by sputtering thin Nb films onto Cu cavities. Copper has a greater thermal conductivity than Nb and is also easier to machine, whilst sputtering films on the surface reduces the amount of Nb used to fabricate the whole cavity. However, sputtering Nb on Cu produces other issues, for example, the surface quality of the Cu affects the quality of the Nb deposited on the surface and therefore the superconducting parameters. As the Nb on the surface is not perfect, the magnetic field produced by the RF can enter the cavity earlier than expected, producing RF losses, which can in turn lead to a quench. One approach is to treat the Nb post deposition by irradiating the surface using a laser to polish the surface of the Nb and increase the surface magnetic field that the cavity can maintain whilst remaining in the Meissner state. A magnetic field penetration experiment designed and built at Daresbury Laboratory has been used to measure the field of full flux penetration to characterise the effect of the laser treatment on the superconducting properties of the Nb. Surface characterisation and the response of the Nb in a DC magnetic field have also been performed to try and provide an explanation for the change in the superconducting properties. The results demonstrate that the laser treatment can lead to an increase in the magnetic field at which the flux penetrates from one side of the sample to the other, thus it could potentially improve the performance of Nb coated RF cavities.**

***Index Terms*—Superconductivity, Magnetic field penetration, Niobium, Type II, Superconducting radio frequency, Laser treatment.**

I. Introduction

Particle accelerators use radio-frequency (RF) to accelerate bunches of charged particles. When the applications of the particle accelerator require high duty cycle or continuous wave operation, superconducting cavities are preferred as they are more efficient. The RF wave has two components; the electric field which accelerates the charged particles (E_{acc}), and the magnetic field (B_{surf}) which is produced perpendicularly to E_{acc}, and therefore applied parallel to the cavity surface.

Superconducting RF (SRF) accelerating cavities are mostly made from bulk Nb. Niobium has one of the largest critical temperature (T_c = 9.25 K) of any element [1], and the largest lower critical field (B_{c1}(0 K) $\approx$ 174 mT) for any known (single element) superconductor [2, 3]. Below B_{c1}, an externally applied magnetic field is expelled from the superconductor due to screening currents present at the surface, and the superconductor behaves as a perfect diamagnet, which is referred to as the Meissner state. Increasing the external magnetic field applied to a Type II superconductor such as Nb increases the supercurrents screening the field, until it becomes energetically favourable for the magnetic field to enter the superconductor in the form of normal conducting cone like structures, called vortices, and is known as the Abriskov state/the mixed state. However, the magnetic field does not necessarily enter the superconductor at B_{c1}. A superconductor can remain in the Meissner state in a metastable regime above B_{c1}, up to the superheating field (B_{sh}) due to the Bean-Livingston surface barrier [4]. The magnetic field can also enter a superconductor below B_{c1} due to defects or impurities on the surface of the superconductor making it energetically favourable for B to enter the superconductor. Under RF conditions, vortices being present in the cavity creates losses in the cavity walls due to the normal conducting regions, and can cause a cavity to quench. Increasing the maximum E_{acc} for SRF applications therefore requires superconductors to remain in the Meissner state to larger B_{surf}. Thus, a major goal for SRF technology is to increase the applied B_{surf} to the superconductors.

One alternative to bulk Nb is to deposit a thin Nb film on a Cu cavity, as the RF only affects a few microns on the surface, typically less than 1 μm [5]. Deposition of Nb has a few benefits compared to bulk Nb cavities, such as;

- Cost - Copper is cheaper than bulk Nb, and the manufacturing costs for Cu cavity are also cheaper than bulk Nb.
- Thermal stability - Cu has a greater thermal conductivity than Nb, creating a smaller temperature gradient from the cavity surface to the liquid He bath. The increased thermal conductivity of the Cu causes the thin film to be more resistant to field emission [5].
- Insensitive to the earths magnetic field [1, 6], so complex magnetic shielding is not required.
- Free from impurities in the Nb, such as steel, nickel and some oxide compounds [5]. These substances can be present within bulk Nb sheets/ingots and can be uncovered by etching, or they can be introduced during the manufacturing process of bulk Nb cavities [7]. Process' can be implemented which remove these impurities, however this increases the manufacturing cost. Deposition under vacuum can avoid adding these impurities.

Manuscript received July 29, 2022; revised September 13, 2022.

Thin film Nb cavities also consist of limitations. For example, the Q-slope (which is also a limiting factor for bulk Nb cavities for high fields) limits thin film cavities to a low E_{acc} [8]. Thin films typically replicate the morphology of the substrate they are deposited on, which alters the RF performance. Additionally, the atoms of the gas used during DC magnetron sputtering can be embedded in the film, which can affect the RF performance of the films [9].

Previous studies have been performed on how the quality of the Cu substrate affects the superconducting performance in a DC magnetic field. A vibrating sample magnetometer (VSM) was utilised to investigate the field of first flux entry (B_{en}) indicating a deviation from perfect conductivity and allowed a comparison in B_{en} between various substrate polishing techniques [10, 11]. Further studies on the affect of substrate polishing have been performed [12] using an in house magnetic field penetration facility (MFPF) designed and built at Daresbury laboratory [13] which applies a local, parallel B from one side of a sample to the other. The MFPF investigates the field of first full flux penetration (B_{fp}), where B has fully penetrated from one side of the sample to the other. Thus, B_{fp} was compared between samples for various substrate treatments. Both systems are described in more detail in sections II-C and II-D.

The structure of the Nb can be altered post deposition by irradiating the sample using laser treatment. Laser treatment has already been performed for bulk Nb [14, 15] and Nb thin films [11, 16, 17, 18]. Previous DC magnetometry tests have been performed on laser treated samples [11, 19, 20] using the conventional VSM technique which showed promising results. However, further studies are required to determine the effect of laser treatment on the superconducting properties of Nb thin films.

The main disadvantage of commercially available magnetometry is that a small sample is placed inside a larger solenoid which applies a B, whereas thin films within a SRF cavity only have B applied from one side. A solenoid produces a uniform B within the coil. However, the presence of a superconducting sample distorts the B lines as B is expelled from the sample, thus producing flux enhancements. Flux enhancements can be accounted for using samples with a well known geometry factor such as spheres or ellipsoids, such that the increased B on the sample surface can be determined [21, 22, 23]. However, if the geometry factor is not known, the local B cannot be determined. Similarly, a planar sample placed on an angle to B will also produce flux enhancements which cannot be accounted for. The samples are mounted into the system by an operator, such that the orientation of the sample with respect to the B may change for each sample, therefore altering the magnitude of any flux enhancement present.

Recently, a new magnetic field penetration facility has been designed and commissioned at STFC Daresbury laboratory. The facility was designed to reduce the limitations present in the VSM. For example, a local, parallel, DC applied magnetic field (B_{app}) is applied from one side of a sample to the other, similar to that in an SRF cavity [13]. As B is applied from one side of a sample (the surface prepared for testing), such that B must enter through the desired surface, i.e.- not the interface between the substrate and the film which is not prepared for RF conditions [13]. A C-shaped magnet applies a constrained B minimising the stray fields produced, therefore removing the possibility of flux enhancement at the sample edges, such that B_{fp} is clear and not influenced by flux enhancements, whilst ensuring easy alignment of B to the sample. In this paper the results obtained using the MFPF on laser treated samples are compared to both untreated samples, and to results obtained with a VSM.

II. Experimental

A. Sample preparation

The Thin Film for Superconducting RF Cavities (TF-SRF) work package (WP15) of the European Union's Horizon 2020 Research and Innovation program under grant agreement no 730871 (ARIES) concentrated on the deposition of Nb thin films on polished Cu substrates. The Cu substrates were cut from 1 mm thick high purity oxygen free high conductivity (OFHC) Cu. Each sample had a surface area of 53×53 mm^2. As the condition of the substrate surface influences the growth of the thin film, and therefore the superconducting properties of the Nb samples, each sample was polished either mechanically, chemically, electrically, or a combination, at CERN or INFN LNL. The surface roughness and reflectivity of the Cu substrates were measured before deposition [10].

TABLE I
THE SUBSTRATE TREATMENT FOR NB COATED THIN FILMS FOR EACH INSTITUTE.

Name	Substrate treatment	Deposition institute	Target thickness [μm]
C7	SUBU CERN	STFC	10
L13	EP	STFC	10
L18	EP + SUBU	STFC	10
L19	SUBU INFN	STFC	10
C1	SUBU CERN	Siegen	3
L1	SUBU INFN	Siegen	3
L9	Tumbling	Siegen	3
L10	EP	Siegen	3
L23	EP + SUBU	Siegen	3
C10	SUBU CERN	INFN	3
L8	Tumbling	INFN	3
L16	EP + SUBU	INFN	3
L20	SUBU INFN	INFN	3
L21	EP	INFN	3

After the substrates had been polished they were sent to one of three institutes; INFN LNL, the University of Siegen or STFC Daresbury Laboratory for deposition. The Nb thin films were deposited by magnetron sputtering, with the set up and deposition conditions previously reported in Refs. [10, 11]. The targeted sample thickness was 3 μm for those deposited at the University of Siegen and INFN, and 10 μm for the samples deposited at STFC Daresbury Laboratory, and are labelled as such throughout. The sample thickness was measured by taking a SEM image of the cross section, with the results for both pre and post laser treatment are shown in Table II. It should be noted that that the error shown in Table II is the statistical error, and not the error in sample preparation

for cross sectional imaging which can produce a discrepancy between the targeted and the measured thickness.

TABLE II
THE MEASURED THICKNESS OF THE NB THIN FILMS AND THE STATISTICAL ERROR OF THE MEASUREMENTS.

Name	Pre-laser treatment [μm]	Post laser treatment [μm]
L1	1.591 $\pm$ 0.009	1.616 $\pm$ 0.057
L10	2.082 $\pm$ 0.204	1.591 $\pm$ 0.025
L13	10.662 $\pm$ 0.928	-
L18	14.242 $\pm$ 0.356	10.780 $\pm$ 0.293

The initial 53$\times$53 mm^2 sample was cut into 2 parts, with dimensions of 53$\times$35 mm^2 and 53$\times$15 mm^2. The larger section of the sample was used for measurements described in Section II-C, whilst the smaller section of the sample was used for measurements in Sections II-B and II-D.

After these initial measurements, the larger section of the films were irradiated using a Nd:YAG laser in an Ar atmosphere with the parameters shown in Table III. The irradiated samples were measured again using the technique presented in Section II-C. After these measurements were completed, the sample was cut again for further testing using the techniques presented in Sections II-B and II-D.

TABLE III
THE PARAMETERS OF ND:YAG LASER USED FOR IRRADIATING THE NB THIN FILMS.

Parameter	Value
Wavelength, λ	1.064 μm
Pulse duration, τ	6 ns
Intensity, I	70 MW/cm^2
Step	5 μm
Dose	66 J/cm^2
Frequency, ν	10 Hz
Beam diameter	3 mm

B. Surface characterisation and morphology

Surface characterisation was performed to correlate the quality of the Nb thin film after laser treatment with the superconducting performance described in sections III-A and III-B. The roughness (R_a) of each sample was measured using a NTEGRA prima atomic force microscope (AFM) in tapping mode with a HA-NC measurement probe from NTMDT spectrum instrument, and was calculated from 3 different spots on each sample surface. The measurements were performed in a 25$\times$25 μm^2 area, using an array of 512$\times$512 scanning points. The AFM measurements were were performed on the same samples pre and post irradiation, however the samples were not tested in the same location for both pre and post laser treatment. The investigated area could have changed on the order of millimeters, whilst the measurements were performed on the order of microns. The surface of the Nb was also investigated by using SEM images, and SEM images were also performed on the cross section of the samples using a FEI quanta 250 FEG scanning electron microscope (SEM). It should be noted that the investigated area of the samples is different pre and post laser treatment for the SEM images. It could be assumed that the surface of the samples are a good representation of the films, however it is unlikely that the samples are perfectly homogeneous. Additionally, investigating the surface of the films provided an insight into the magnetometry measurements.

Samples deposited at same institute exhibit similar effects due to laser treatment, therefore only a few images are provided in the paper. The three samples deposited at STFC (C7, L13, L18, with L18 shown in Fig. 1a and 2b) show well grown Nb crystals post laser treatment, which is likely due to re-crystallisation. This is expected to be due to the laser rapidly heating the surface layers of Nb, which form large grain crystals upon cooling. Additionally, the number of cracks present on the surface of the samples seem to have reduced, however this could also be due to the change in scale used to take the images.

The Nb thin films deposited by the University of Siegen have a different surface morphology. The surfaces for some samples deposited at Siegen are shown in Figure 1. There are no visible presence of grain boundaries with a 10 μm scale, with some small bumps present on the samples. It can be seen in Figs. 1e and 1d that the sample roughness is reduced due to the laser treatment, and scratches in the surface are also slightly reduced. However, it can be seen in Figs 1e and 1f that the surface of the films have also been damaged, indicated by cracks on the most damaged samples. This damage is likely caused by the heat generated by the laser being deposited in the Cu substrate rather than the Nb film. The parameters of the laser were kept consistent, and therefore the deposition depth of the laser was also consistent. However, there is a visible difference of the surface between the samples deposited at STFC and the University of Siegen, with the film thickness being the main difference between institutes. Thus, for the thinner Nb films it is thought that the heat produced by the laser was deposited into the Cu substrate instead of the Nb. Thus, due to the Cu substrate possessing a greater thermal conductivity than Nb, the Cu substrate expanded faster than the Nb film. The expansion of the substrate therefore produced a force on the film (due to the film possessing a smaller coefficient of thermal expansion), in turn generating tensile stress between the superconducting film and the substrate. If the force on the film became large enough due to the substrate, the film would be damaged. Alternatively the cracks on the surface could have also been produced due to rapid solidification of the liquid metal, which has been observed in other metals which have been laser treated [24, 25].

Additionally, at the top right of Fig. 1f shows some dark holes which look like subsurface heating has taken place, also known as the lid effect [26]. Subsurface heating is where the Cu substrate melts underneath the Nb film, and due to the rapid thermal expansion of the Cu breaks through the Nb film. The expanding molten Cu can therefore produce holes in the Nb film allowing B to penetrate the sample early.

Cross sectional SEM imaging was also performed on samples L1 and L10 deposited at the University of Siegen, and L13 and L18 deposited at STFC, with a comparison for before and after laser treatment shown in Fig. 2 for sample L1 and L18. The cross-sectional images also indicate that the microstructure of the Nb films were similar for each institute,

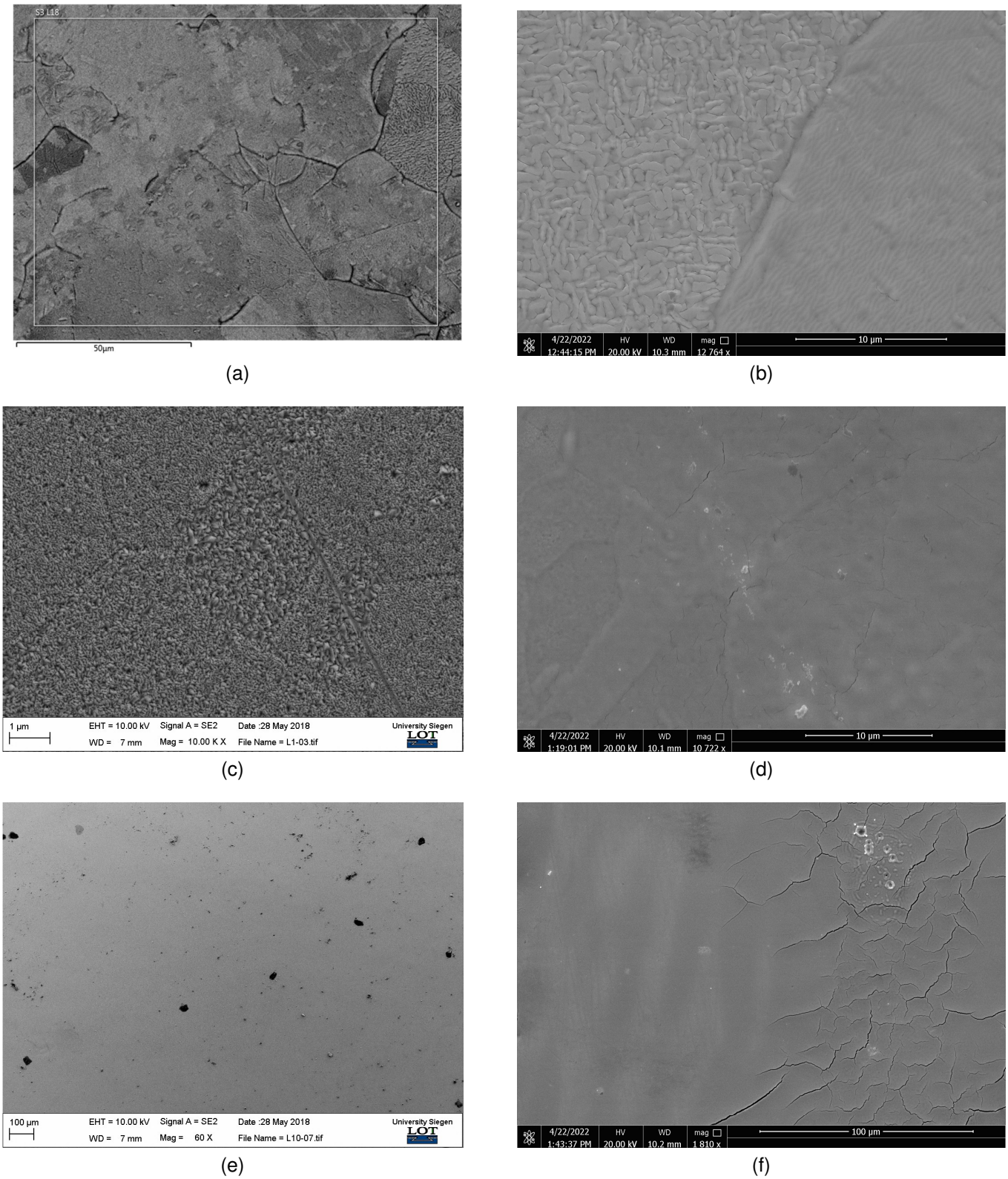

(a) (b) (c) (d) (e) (f)

Fig. 1. The surface SEM images for samples deposited at STFC Daresbury Laboratory and the University of Siegen, before laser treatment (left) and after laser treatment (right) for samples L18 (1a, 1b), L1 (1c, 1d), and L10 (1e, 1f)).

i.e. samples L1 and L10 had a similar structure, as did L13 and L18. However the microstructure for the Nb films is different between STFC and University of Siegen. None of the investigated samples microstructure changed due to the laser treatment, however R_a was reduced in all samples. For both samples it can be seen that the Cu substrate underneath the Nb film has melted. Additionally, Fig. 2d looks as if the Cu has entered, and possibly broken through the Nb thin film

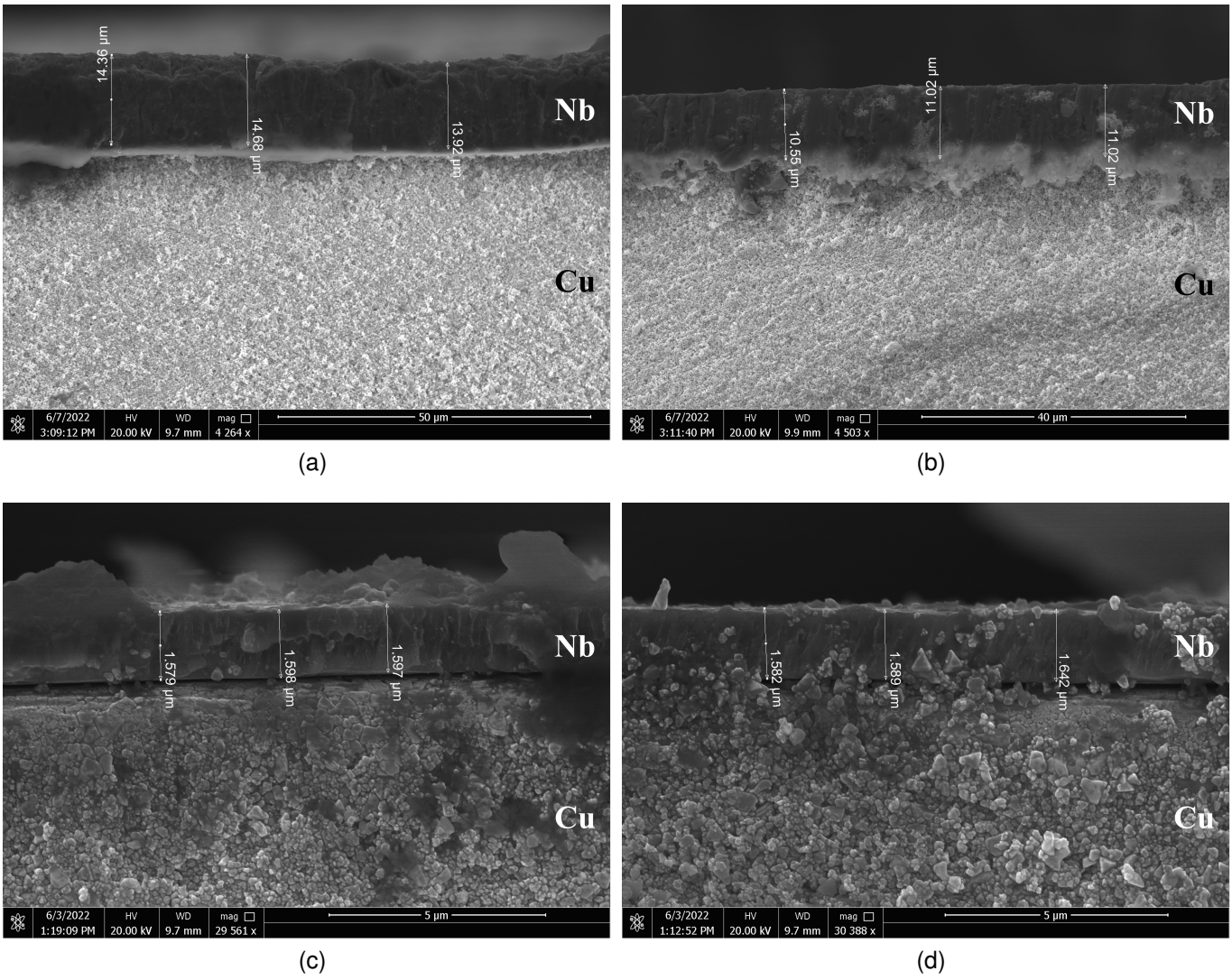

Fig. 2. The cross-sectional SEM images of samples L18 (10 μm deposited at STFC) pre-laser treatment (2a) and post laser treatment (2b), and L1 (3 μm deposited at the University of Siegen) pre-laser treatment (2c) and post laser treatment (2d).

- the lid effect [26].

Figure 3 shows the surface for the AFM measurements and the corresponding roughness of samples L18 and L1 both pre and post laser treatment. The images are of the same samples both pre and post laser treatment, however not the same local area on the sample surface will have been investigated. The measurements were repeated at various areas of the sample, which produced similar results. The R_a decreased for all samples post laser treatment. Sample L18 had one of the largest reductions in R_a, from a mean R_a value of 69.2 nm to 40.1 nm due to laser treatment. Sample L1 had a lower mean R_a of 24.9 nm than L18 due to irradiation, however they are comparable.

C. Magnetic field penetration facility

A MFPF has been designed and built at STFC Daresbury laboratory [13] which determines the field of full flux penetration (B_{fp}), which is the parallel B_{app} from one side of the sample which has fully broke through to the opposing side of the sample. This is not the same as B_{c1}. This is because B_{fp} is the applied field at which the flux has penetrated all the way through the sample, from one side of the sample to the other, whereas B_{c1} is the magnetic field at which it is energetically favourable for B to enter the sample. It should be noted that for thick Type II superconductors, vortices can enter from one side of the sample and leave on the same side of the sample and cannot be detected. Thus, the flux forms a semi-loop within the superconductor [27, 28].

The MFPF uses low temperature superconducting solenoid to generate a magnetic field, and a C-shaped ferrite yoke with a 2 mm gap in which B_{app} is generated parallel to the sample surface, denoted by B_1. A small gap constrains B_1, which limits edge effects that can be generated on the sample. Two Hall probe sensors are used to measure the magnetic field in the facility. Hall probe 1 (HP1) measures B_1, and Hall probe 2 (HP2) measures the magnetic field on the opposing side of the sample (B_2). A cross section of a simulation of the magnet with a current of 1 A is shown in Fig. 4a, with the position of

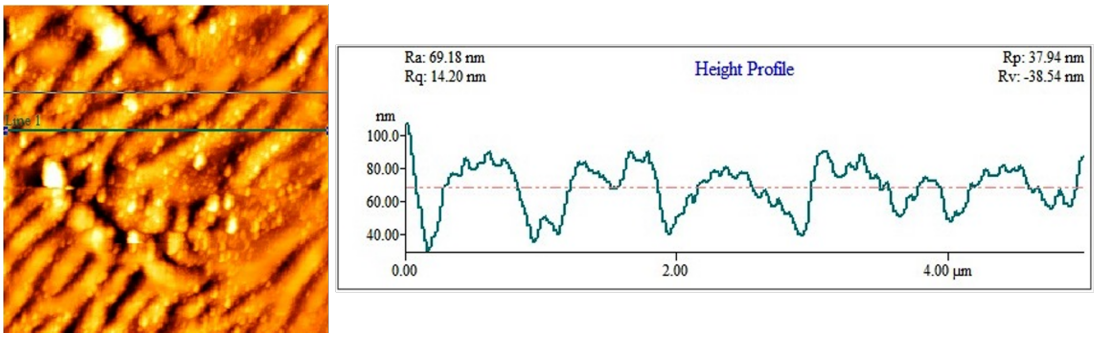

(a)

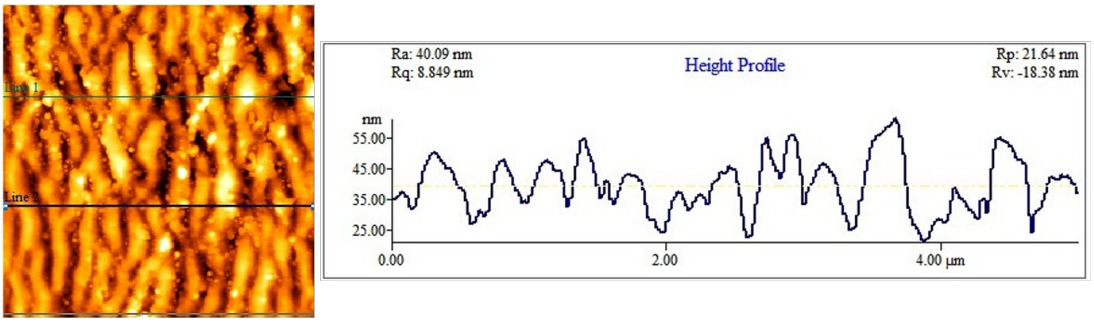

(b)

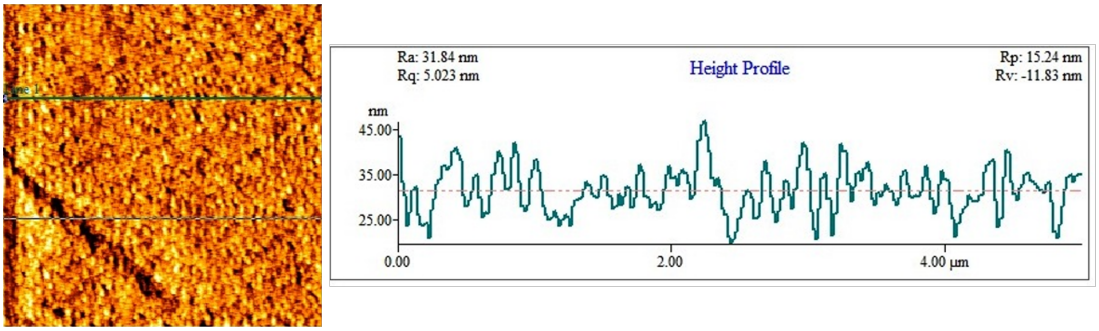

(c)

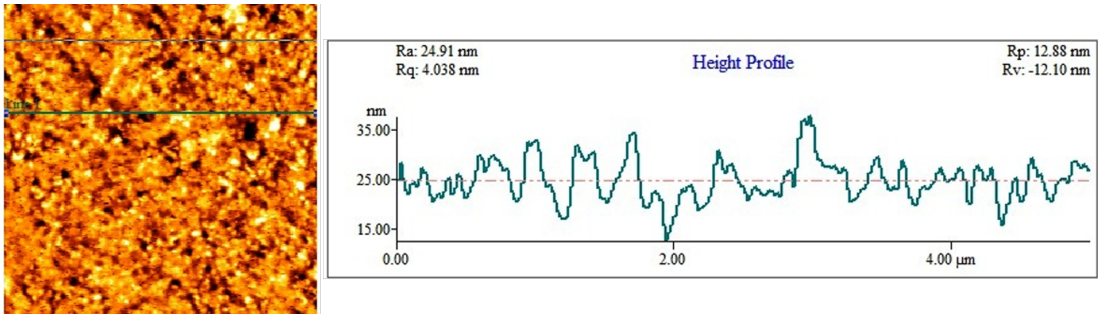

(d)

Fig. 3. The AFM measurements of samples L18 (10 μm deposited at STFC) pre-laser treatment (3a) and post laser treatment (3b), and L1 (3 μm deposited at the University of Siegen) pre-laser treatment (3c) and post laser treatment (3d). The colour of the line indicates the position of the measurements on the sample. Multiple measurements were taken at different areas to ensure consistent results.

the sample and the Hall probe sensors also shown. In addition, the physical system is shown in Fig. 4b.

The sample undergoes ZFC for each test to ensure no flux is trapped within the sample. Increasing the current applied to the solenoid increases B_1. The magnetic field at which B_1 has penetrated from one side of the sample to the other (determined by a rapid increase in B_2) is defined as B_{fp}, and is determined to be the greatest rate of change in $d^2(B_2)/d(B_1)^2$.

The facility measures B_{fp} at multiple set temperatures,

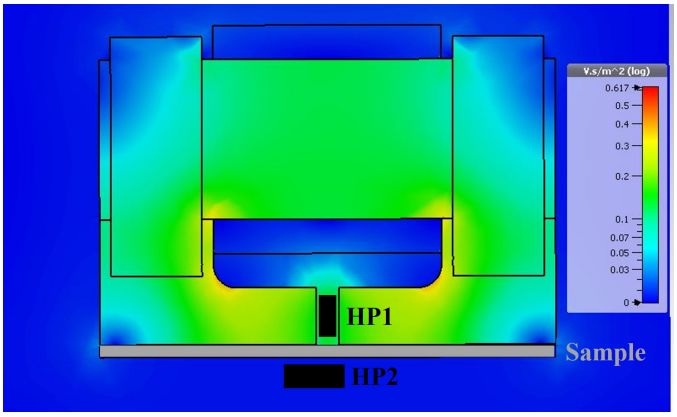

(a)

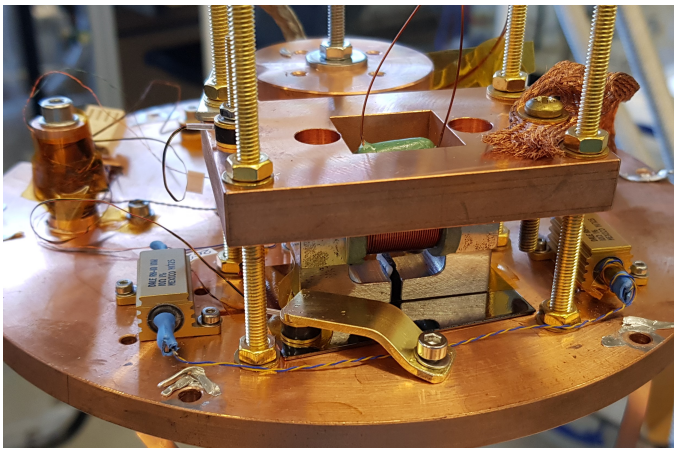

(b)

Fig. 4. (a) A cross-sectional view of the MFPF set up, with the positions of the Hall probe sensors shown with respect to a sample and the magnet (b) The set up of the MFPF with a 3 μm Nb thin film.

which is controlled using a PID loop and heaters placed either side of the sample. After each set temperature run, the sample is heated above the T_c of the sample and held for 15 minutes for temperature stabilisation and to ensure any and all trapped flux is removed from the film, before undergoing a ZFC to the next temperature set point. Further information about this facility can be found in Ref. [13]. An example of raw data produced by the MFPF is shown in Fig. 5 for multiple temperatures for sample C7.

D. Vibrating sample magnetometry

The superconducting properties of the samples have also been studied using conventional DC magnetometry techniques. The Nb thin films were measured in a VSM, integrated in a commercial Physical Property Measurement System (PPMS) from Quantum Design Inc. at the Institute of Electrical Engineering[11, 29]. Small samples of approximately 2×2 mm^2 cuboids were cut from the original 53×35 mm^2 samples, and then placed in a uniform B_{app} applied either parallel or perpendicular to the flat face of the superconducting thin film.

After cooling the sample below T_c in zero applied field (zero field cool-down, ZFC), the initial magnetization curve was measured increasing the applied field from 0 up to a maximum value B_{max}, at a constant rate. From this point the measurement continued performing a hysteresis loop, ramping the applied field from B_{max} to $-B_{max}$ and back to B_{max}. All measurements conducted in a varying B_{app} were performed at a constant temperature at 4.22 K.

Whilst the sample is in the perfect shielding conditions of the Meissner state, the magnetic moment (m) is proportional to B_{app} and the initial magnetization curve is thus linear (due to the Meissner state) at low B_{app}. Above a certain value of the applied field, proportional to the first critical field B_{c1} through a geometrical constant, the magnetic flux starts penetrating inside the superconductor, reducing the total superconducting volume and consequently decreasing the absolute value of the magnetic moment. This defines the so-called field of first magnetic flux entry, B_{en}. Whilst the geometry factor can be well defined for spherical and ellipsoidal samples, it is much more difficult to determine for flat samples. The flux enhancements present on the surface of the film are influenced by the angle of the film to B_{app}, which cannot be accurately measured for small samples when mounted in the VSM.

It should be noted that B_{en} and B_{fp} are not the same. The B_{en} is the first flux entry into a superconducting material, whereas B_{fp} is the field which has fully penetrated from one side of a superconductor to the other. However, in realistic samples, flux pinning is usually present (to some degree). In such a case, the start of the flux penetration does not generate any distinct feature on the initial magnetization curve. The curve deviates smoothly from the linear Meissner slope towards smaller absolute values of m, as shown in Fig. 6 for the laser treated films. We have thus determined B_{en} from the initial magnetization curves employing an arbitrary 2% relative difference criterion between the linear Meissner slope and the measured initial curve.

The critical temperatures were determined from the temperature dependence of the magnetic moment, m(T), at a constant B_{app}. At a temperature well above the T_c a small constant magnetic field (typically 5 mT) was applied to a sample, which was then slowly cooled down with the field still present to determine the temperature at which there is a sudden change in the magnetic moment, indicating the superconducting transition. For simplicity, the reported T_c was determined as the onset of the increase in the absolute m with decreasing temperature.

III. Results

A. Magnetic field penetration facility

A summary of the results obtained the MFPF both before and after laser treatment are shown in Table IV to compare B_{fp} for samples deposited on substrates polished by various techniques, and deposited at three institutes. The first round of testing has been presented in Ref. [12], however the data analysis technique has been improved upon which is further described in Ref. [13] such that the results are slightly different.

The samples deposited at STFC are thicker than the samples deposited at the other two institutes, which increases B_{fp} [13]. The samples deposited at INFN were not tested by the MFPF

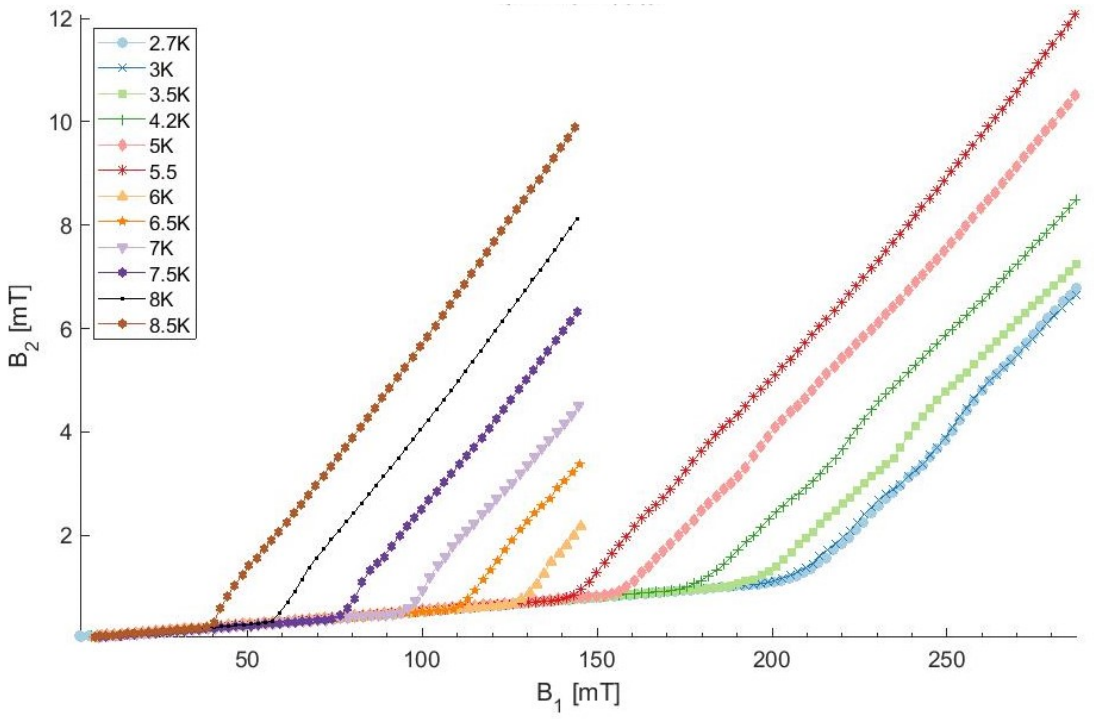

Fig. 5. The raw data produced by the MFPF run at multiple temperatures for a 10 μm Nb thin film on sample C7 after the laser treatment of the Nb film.

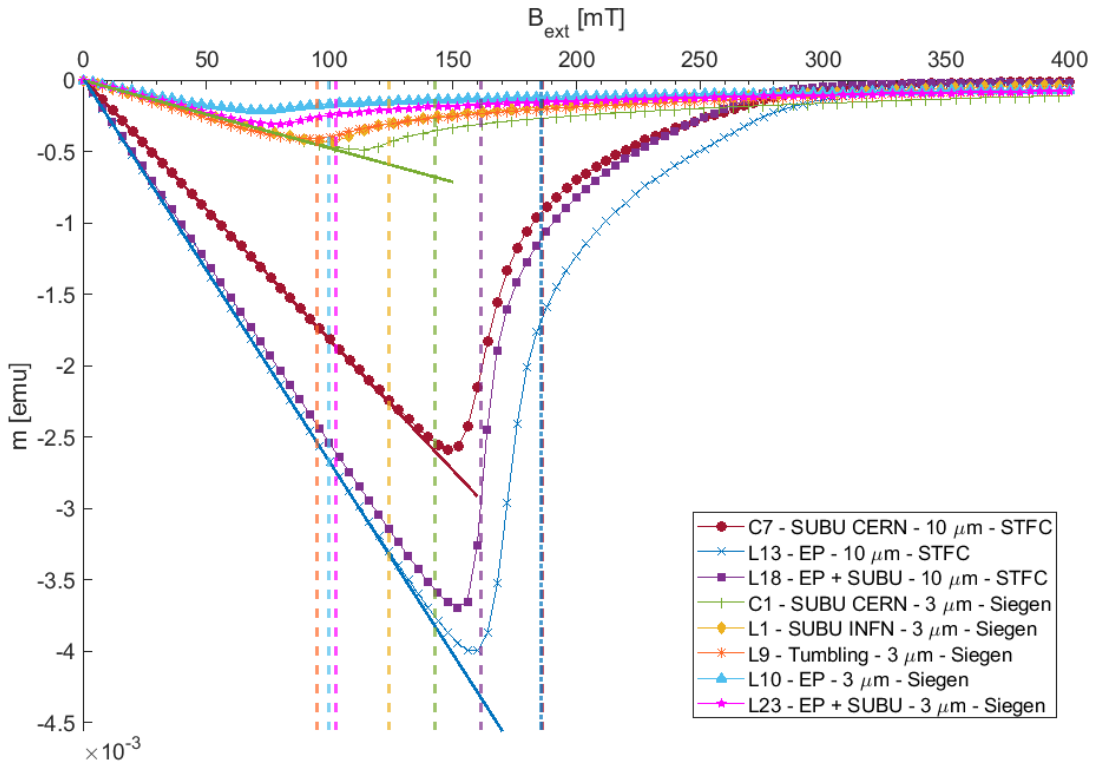

Fig. 6. The initial magnetisation curve produced by the VSM for the laser treated films, all performed at 4.2 K. The Meissner line is shown for samples C1, C7 and L13.

before irradiation, so there is no comparison for the change in B_{fp} due to irradiation, and whilst almost all samples were tested at 4.2 K to determine B_{fp}, the samples that were not tested at 4.2 K have been calculated using the line of best fit using the linear dependence of B_{fp} as a function of T^2. Finally, the first round of samples (laser treated Nb films deposited at INFN and non-laser treated Nb films deposited at Siegen and STFC) have measurements approximately 1 K

TABLE IV
THE B_{fp} MEASURED AT 4.2 K. FOR SAMPLES NOT MEASURED AT 4.2 K THE EXPECTED VALUE FOR B_{fp} HAS BEEN EXTRAPOLATED USING A LINEAR DEPENDENCE OF B_{fp} AS A FUNCTION OF T^2 WHICH IS DENOTED BY '*'. THE B_{fp} AS A FUNCTION OF T^2 HAS ALSO BEEN USED TO EXTRAPOLATE T_c.

	Pre-Laser Treatment		**Post-Laser Treatment**		**Change due to laser treatment**	
	B_{fp}**(4.2K) [mT]**	T_c **[K]**	B_{fp}**(4.2K) [mT]**	T_c **[K]**	ΔB_{fp}**(4.2K) [mT]**	ΔB_{fp}**(4.2K) [%]**
C7	174.4 ± 2.6*	9.19 ± 0.11	186.3 ± 0.8	9.18 ± 3.4	+10.5	+6.0
L13	177.0 ± 1.1	9.61 ± 0.08	185.8 ± 0.5	9.19 ± 0.08	+8.8	+5.0
L18	152.0 ± 2.8*	9.29 ± 0.07	161.2 ± 0.4	9.55 ± 0.03	+9.2	+6.1
L19	163.1 ± 1.4*	9.31 ± 0.03	-	-	-	-
C1	127.7 ± 4.8*	9.38 ± 0.13	142.8 ± 0.7	9.24 ± 0.06	+15.1	+11.8
L1	137.5 ± 1.1	9.73 ± 0.07	123.8 ± 0.7	9.75 ± 0.06	-13.7	-10.0
L9	116.0 ± 0.8	9.10 ± 0.11	102.7 ± 0.4	8.92 ± 0.10	-13.3	-11.5
L10	137.8 ± 6.6	9.57 ± 0.12	94.7 ± 0.4	8.98 ± 0.92	-43.1	-31.3
L23	100.4 ± 1.1	8.95 ± 0.13	99.8 ± 0.4	8.90 ± 0.90	-0.6	-0.6
C10	-	-	140.6 ± 4.0*	9.30 ± 0.10	-	-
L8	-	-	165.9 ± 4.4	9.67 ± 0.09	-	-
L16	-	-	116.9 ± 6.2*	9.17 ± 0.20	-	-
L20	-	-	142.9 ± 8.7*	9.36 ± 0.30	-	-

apart, whereas the more recent measurements (laser treated Nb deposited at Siegen and STFC) were performed approximately every 0.5 K, as the system became automated and remotely operated, which removed time as a limiting factor for measurements.

The MFPF tests samples at a range of temperatures, however to allow a comparison to the VSM the data for B_{fp}(4.2 K) is shown in Table IV. A linear relation for $B_{fp}(T^2)$ was found, such that $B_{fp}(T^2) = Gradient \times (T^2) + B_{fp}(0K)$. Extrapolating the line of best fit until $B_{fp}(T^2) = 0$ mT allows T_c for the sample to be estimated, and also extrapolating until T^2 = 0 K allows $B_{fp}(0K)$ to be found. This linear relationship therefore allows B_{fp} to be estimated at various T values, such as at 4.2 K shown in Table IV. The error in these values are found using the equation $\Delta B_{fp}(T^2) = \left[\left((\Delta Gradient)^2 \times (T^2)\right) + (\Delta B_{fp}(0K))^2\right]^{1/2}$.

The results produced by the MFPF show that the samples deposited at STFC show an enhancement in B_{fp} up to 10 mT, indicating that the laser treatment has had a similar effect on all samples. Samples C7 and L13 (SUBU polishing at CERN and electro-polishing) have a similar B_{fp} post laser treatment, which could indicate the laser treatment has altered the surface such that both samples are have a similar structure. The EP + SUBU sample for STFC (L18) still has the lowest B_{fp} for all the samples post laser treatment, similar to pre-laser treatment.

The largest increase in B_{fp} for all samples is sample C1, the Nb sample deposited on a Cu substrate polished at CERN using the SUBU technique, with an increase of 15.1 mT to the pre-laser treated sample. However, this sample contradicts the other 4 samples deposited at Siegen which all saw a decrease in B_{fp}. Samples L1 and L9 (SUBU polishing performed at INFN and tumbling) saw a similar decrease in B_{fp} by ≈13 mT, whereas L10 (the electro-polished Cu substrate) which previously produced the largest B_{fp} for all the samples deposited at Siegen, had the greatest drop in B_{fp} by 43 mT, causing it to produce the lowest B_{fp} for all the samples deposited at Siegen even pre-laser polish.

The samples deposited at Siegen with laser treatment produce similar results to the samples deposited at INFN with post laser treatment. It could be assumed that if the effect of laser treatment is due to the thickness of the sample, there would be a similar effect on the samples from both INFN and Siegen, and this would explain the increase in B_{fp} for all samples deposited at STFC. If the effect of the laser treatment was due to the type of substrate polishing, it would be expected that each polishing technique would alter B_{fp} a similar way for each deposition institute.

The results produced by the MFPF show that thicker Nb films deposited at Daresbury Laboratory had an increase in B_{fp}, whereas the thinner films deposited at Siegen have an overall reduced B_{fp}. One explanation for this is possible melting or boiling of the Cu substrate under the Nb film, known as subsurface melting or the lid effect [26]. As the rapid expansion of the Cu substrate due to increased thermal conductivity of the Cu could be an explanation for damage of the Nb films on the surface which do not expand as fast. The expanding molten Cu can create holes in the Nb which will create holes which will allow B_{app} to penetrate through the sample early. For the thicker samples deposited at STFC, this may not be the case. Heat produced due to the irradiation would be deposited in the Nb film rather than the Cu substrate, which has a lower thermal conductivity. Therefore subsurface heating would not be present, and the Nb film would not expand due to heating as quick as Cu such that the film is not damaged. To determine if the enhancement in B_{fp} produced by irradiation is due to the thickness of the Nb films a further study must be conducted with a range of samples of varying thickness.

B. Vibrating sample magnetometer

To determine the quality of the superconducting thin films small samples were cut and tested in the VSM, measuring T_c and B_{en}, with B_{app} in both the parallel and perpendicular orientation (B_{para} and B_{perp} respectively), and have previously been presented in [10, 11, 29]. The data is also presented

TABLE V
THE $B_{en}(4.2K)$ AND $T_c(5mT)$ FOR NB THIN FILMS ON CU SUBSTRATE WITH VARYING POLISHING METHODS, FOLLOWED BY POST DEPOSITION LASER TREATMENT ON THE NB SURFACE. THE ERROR IN $B_{en}(4.2K)$ IS 5% FOR EACH MEASUREMENT.

	Pre-Laser Treatment			**Post-Laser Treatment**			**Change due to laser treatment**		
	$B_{en,perp}$ **[mT]**	$B_{en,para}$ **[mT]**	T_c**[K]**	$B_{en,perp}$ **[mT]**	$B_{en,para}$ **[mT]**	T_c**[K]**	$B_{en,perp}$ **[mT]**	$B_{en,para}$ **[mT]**	ΔB_{en}%
C7	24.1	150.1	9.35	-	139.0	9.23	-	-11.1	-7.4
L13	22.0	100.3	9.35	-	144.0	9.24	-	+43.7	43.6
L18	17.7	61.0	9.30	-	143.0	9.22	-	+82.0	134.4
L19	17.3	73.2	9.20	-	-	-	-	-	-
C1	15.5	49.6	9.50	-	83.0	9.28	-	+33.4	67.3
L1	14.5	38.0	9.60	-	83.0	9.27	-	+45.0	118.4
L9	16.0	38.6	9.38	-	59.0	9.30	-	+20.4	52.8
L10	15.5	32.7	9.38	-	37.0	9.16	-	+4.3	11.4
L23	15.0	24.5	9.38	-	43.0	9.14	-	+18.5	75.5
C10	12.0	-	9.37	17.0	50.2	-	+5.0		41.7
L8	18.0	-	9.48	19.1	42.5	-	+1.1	-	6.1
L16	14.0	-	9.37	15.5	47.2	-	+1.5	-	10.7
L20	20.0	-	9.58	23.7	450	-	+3.7	-	18.5
L21	18.0	-	9.28	18.8	45.2	-	+0.8	-	4.4

in Table V to allow comparison with after the samples have been irradiated. A few things should be noted; the samples deposited at STFC are thicker than the other 2 institutes (10 μm compared to 3 μm) and therefore lead to an increased m which is visible in Fig. 6. The samples deposited at INFN were only tested in the B_{perp} configuration pre-laser treatment so the post laser treatment results can only be compared in the same field orientation, and the 'L19' sample did not undergo laser treatment due to being used in an alternative experiment.

The VSM determined there was an increase in B_{en} for every sample except one, the Nb deposited at STFC on a Cu substrate polished by chemical polishing at CERN, C7. Pre-laser treatment, C7 had the largest B_{en} for B_{para}, suggesting the sample could have induced damage during the laser treatment and therefore reducing the superconducting performance. The other 2 samples deposited at STFC show a large increase of 43.7 and 82.0 mT in B_{en} for B_{para}.

All samples deposited at Siegen show an increase in B_{en}, with the Nb film on the Cu substrate chemical polished at INFN (L1) gaining the largest increase. After irradiation B_{en} is the same for both chemically polished substrates (C1 and L1) in the B_{para} configuration.

Samples deposited at INFN also all shown an increase in B_{en} due to irradiation, however they were only tested in the B_{perp} configuration. Each sample shows an increase in B_{en}, but much smaller than the samples deposited at the other 2 institutes due to normal components of B applied to the film surface entering the sample much earlier. It can be expected that if there is an increase in B_{en} in the B_{perp}, then there should be an increase in the B_{para} configuration also.

Comparing the T_c both before and after laser treatment shown in Table V, it can be seen that the critical temperature also changes to values much closer to the expected T_c of Nb[2], however this could also be due to a change in the measurement parameters as the temperature ramp rate was reduced and more points were taken for the laser treated films.

However, the VSM suffers some technical issues. As the sample is placed in a B with a geometry larger than the sample, edge effects can cause B to enter the sample early as B_{app} is enhanced at the edges of the sample, therefore causing early B_{en}. In addition, when trying to align a sample it is possible that the sample is not perfectly parallel with B_{app} and a normal component of the magnetic field will be present, which can also cause early B_{en}. Finally, as small samples have had to be cut to fit inside the VSM, impurities can be introduced to the samples from the machining tools, which again can cause early B_{en}. Therefore, it is possible that the change in B_{en} that initially looks due to irradiation could be due to a change in any of the aforementioned issues when the sample is placed in the system, and it is difficult to ensure that B_{en} is a physical superconducting property, or if this is due to a number of other effects present due to the type of measurement.

IV. DISCUSSION

In total, 14 Nb thin films were deposited on Cu substrates which were polished by different techniques, and were analysed as part of the ARIES collaboration using a MFPF and a VSM. The samples were then irradiated using a laser at Riga Technical University, followed by further analysis of the samples using 2 DC magnetometry techniques. These techniques do not investigate the same properties. The VSM measures the total superconducting volume, and can determine B_{en} and is highly sensitive to this property, whereas the MFPF investigates B_{fp}. The main difference is that vortices can enter and leave from the same side of the sample which cannot be detected by the MFPF.

Measurements in the MFPF determined that samples with the same polishing technique do not produce a consistent change in B_{fp} for each institute i.e - EP samples do not increase the same amount for each deposition institute once they have been irradiated. It can therefore be determined that whilst the effect of polishing is critical to ensure a high quality film is grown on the substrate, it does not affect the outcome once the sample is irradiated by laser treatment withing the uncertainty of the study.

The irradiation of the Nb reduces the surface roughness as the Nb 'hills' flows into the 'valleys', thus producing a more

homogeneous film thickness. It is possible that prior to laser treatment the smaller values for B_{fp} was due to the applied B breaking through local areas of reduced thickness. Thus, irradiating the sample increased the minimum thickness of the films, thus increasing B_{fp}, as B_{fp} is thickness dependant [13]. Although the thickness of the Nb is reduced due to the irradiation, it is not expected to have a large influence on B_{fp} as the change in thickness is not on the order of μm.

Measurements produced in the VSM in Bratislava show an increase in B_{en} for all samples that have been irradiated except the Nb film deposited by STFC on SUBU polished substrate at CERN. Whilst the increase in B_{en} can be due to laser irradiation, it is possible that the increase in B_{en} could be due to a number of reasons such as flux enhancements or normal components present in previous tests, which have then been improved upon in further rounds of testing, which makes the latter rounds appear to have improved qualities due to laser treatment. The Nb films were placed in a uniform B_{app}. In the Meissner state, the film disturbs B_{app} such that localised flux enhancements are generated on the the film. Flux enhancements can be accounted for using a demagnetisation factor for well known samples such as ellipsoids or spheres, however the films were mounted into the system by an operator such that the angle of the film with respect to the B may change for each film, thus altering the magnitude of any flux enhancement present. Hence, the flux enhancements in the VSM were not accounted for.

However, thick samples produce an increase in B_{fp} in the MFPF, whilst all 3 μm thick samples except one show a decrease in B_{fp}, and it is likely that the effect of thickness is the main cause for an increased B_{fp}. Further studies should be performed to determine how post deposition laser treatment varies as a function of thickness.

The cross-sectional SEM images show that the microstructure of the Nb does not change due to laser treatment, and the Cu substrate has melted due to the heat from the laser. The parameters of the laser are kept constant, thus the penetration depth is also constant. In this case, the heat deposited by the laser can produce different effects for different areas of the sample, due to different thickness' and initial surface roughness. For example, samples at STFC are thicker, and therefore all of the heat may be deposited in the Nb, producing localised annealing and reducing the surface roughness. However, if the samples are thinner than the penetration depth of the laser, such as the samples deposited at Siegen, the energy could be deposited at the Nb/Cu boundary, melting both the film and the substrate and allowing them to mix, or even break through the superconducting film. Finally, if the energy is deposited in the Cu substrate only, the heating and enhanced thermal conductivity of the Cu allows the substrate to expand. The expansion can then generate stress between the substrate and the thin film, which leads to the film becoming damaged.

By comparing the results between B_{en} produced by the VSM and B_{fp} produced by the MFPF leads to the conclusion that there is some correlation between both $B_{en}(4.2K)$ and $B_{fp}(0K)$, where samples with a greater B_{en} also have produce a greater B_{fp}, shown by the line of best fit in Fig. 7. Thus, the samples deposited at STFC are situated towards the top right of Fig. 7, and the samples deposited by Siegen are shown on the lower left. For future thick samples, it can be expected that if a superconducting sample performs well in one facility, it is likely to perform well in the other.

All samples saw a reduction in R_a after laser treatment. However there was no correlation between the surface roughness and B_{fp}. The samples deposited at STFC had a lower R_a than the samples deposited by the university of Siegen, except for the exception of sample C7. Sample C7 produced the largest B_{fp} whilst having a roughness similar to that of the samples produced at Siegen. However, the surface roughness (and the surface analysis) were performed on small $2\times2\text{mm}^2$ samples from the edge of the original sample. Therefore whilst surface characterisation produce an insight into the quality and structure of the Nb thin films, it does not necessarily represent the area probed by the MFPF, as they are two different areas.

V. Conclusion

Comparative studies of superconducting properties have been performed using MFPF and a VSM techniques on 14 Nb thin films coated onto polished Cu substrates.

There are two main conclusions. There is a correlation between the results obtained with MFPF and VSM. For samples with a higher B_{fp} in the MFPF tend to produce to higher B_{en} in the VSM. The results demonstrate that laser treatment can provide higher B_{fp} (and therefore B_{en}) measurements, thus it could also potentially improve performance of Nb coated RF cavities.

VI. Acknowledgments

This research has been supported by European Commission's ARIES collaboration H2020 Research and Innovation Programme under Grant Agreement no. 730871. This work was conducted under the aegis of the Science and Technology Facility Council (STFC). For the purpose of open access, the author has applied a Creative Commons Attribution (CC BY) licence [where permitted by UKRI, 'Open Government Licence' or 'Creative Commons Attribution No -derivatives (CC BY-ND) licence' may be stated instead] to any Author Accepted Manuscript version arising.

The authors would like to acknowledge the cryolab technicians J. Conlon and L. Smith for their daily help and technical support.

References

[1] H. Padamsee, J. Knobloch, and T. Hays, "Rf superconductivity for accelerators," *New York. A Wiely-Interscience Publication*, pp. 129–144, 1998.

[2] D. Finnemore, T. Stromberg, and C. Swenson, "Superconducting properties of high-purity niobium," *Physical Review*, vol. 149, no. 1, p. 231, 1966.

[3] T. Junginger *et al.*, "Field of first magnetic flux entry and pinning strength of superconductors for rf application measured with muon spin rotation," *Physical Review Accelerators and Beams*, vol. 21, no. 3, p. 032 002, 2018.

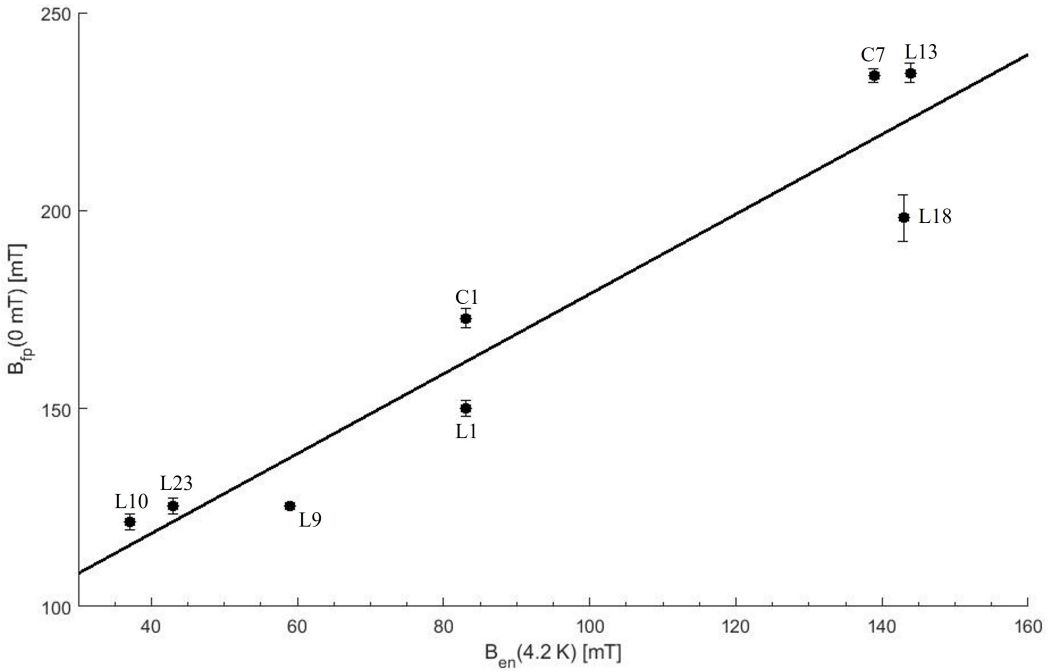

Fig. 7. A comparison between the $B_{fp}(0K)$ produced by the MFPF and $B_{en}(4.2K)$ produced by the VSM for all samples post laser treatment.

[4] C. Bean and J. Livingston, "Surface barrier in type-ii superconductors," *Physical Review Letters*, vol. 12, no. 1, p. 14, 1964.

[5] A.-M. Valente-Feliciano, "Superconducting rf materials other than bulk niobium: A review," *Superconductor Science and Technology*, vol. 29, no. 11, p. 113 002, 2016.

[6] T. Wang, C. Reece, and R. Sundelin, "Dc field emission studies on nb," Thomas Jefferson National Accelerator Facility, Newport News, VA (US), Tech. Rep., 2001.

[7] C. Durand, W. Weingarten, P. Bosland, and J. Mayer, "Non quadratic rf losses in niobium sputter coated accelerating structures," *IEEE Transactions on Applied Superconductivity*, vol. 5, no. 2, pp. 1107–1110, 1995. DOI: 10.1109/77.402745.

[8] V. Palmieri and R. Vaglio, "Thermal contact resistance at the nb/cu interface as a limiting factor for sputtered thin film rf superconducting cavities," *Superconductor Science and Technology*, vol. 29, no. 1, p. 015 004, 2015.

[9] C. Benvenuti *et al.*, "Study of the surface resistance of superconducting niobium films at 1.5 ghz," *Physica C: Superconductivity*, vol. 316, no. 3, pp. 153–188, 1999, ISSN: 0921-4534. DOI: https://doi.org/10.1016/S0921-4534(99)00207-5.

[10] C. Pira *et al.*, "Evaluation of cleaning process, aries delivery report d15.1," *Horizon 2020 Research Infrastructures*, 2018.

[11] C. Pira *et al.*, "Impact of the cu substrate surface preparation on the morphological, superconductive and rf properties of the nb superconductive coatings," *in Proceedings of SRF*, 2019.

[12] D. Turner and et al, "Magnetic field penetration of niobium thin films produced by the aries collaboration," in *Proc. SRF 2021*, 2021, SUPFDV007.

[13] D. A. Turner, O. B. Malyshev, G. Burt, T. Junginger, R. Valizadeh, and L. Gurran, "A facility for the characterisation of planar multilayer structures with preliminary niobium results," *Superconductor Science and Technology*, 2022.

[14] A. Cubero *et al.*, "Effects of laser-induced periodic surface structures on the superconducting properties of niobium," *Applied surface science*, vol. 508, p. 145 140, 2020.

[15] L. Zhao, J. M. Klopf, C. E. Reece, and M. J. Kelley, "Laser polishing for topography management of accelerator cavity surfaces: Laserpolieren als topographiemanagement zur schnellen herstellung von oberflächen mit mulden," *Materialwissenschaft und Werkstofftechnik*, vol. 46, no. 7, pp. 675–685, 2015.

[16] E. Radicioni, C. Benvenuti, M. Bianconi, and L. Correra, "Laser annealing of nb coatings for superconducting rf accelerating cavities," *Nuclear Instruments and Methods in Physics Research Section A: Accelerators, Spectrometers, Detectors and Associated Equipment*, vol. 365, no. 1, pp. 28–35, 1995.

[17] A. Medvids *et al.*, "Improvement of nb/cu adhesion and increase of nb crystal size by laser radiation," *Applied Surface Science*, vol. 525, p. 146 528, 2020.

[18] Y. Yang, X. Lu, W. Tan, L. Xiao, L. Zhu, and D. Xie, "Study on laser annealing of niobium films deposited on copper for rf superconducting cavities," *Nuclear Instruments and Methods in Physics Research Section A: Accelerators, Spectrometers, Detectors and Associated Equipment*, vol. 964, p. 163 803, 2020.

[19] R. Ries *et al.*, "Improvement of the first flux entry field by laser post-treatment of the thin nb film on cu," *Superconductor Science and Technology*, vol. 34, no. 6, p. 065 001, 2021.

[20] R. Ries, E. Seiler, F. Gömöry, A. Medvids, C. Pira, and O. Malyshev, "Superconducting properties and surface roughness of thin nb samples fabricated for srf applications," in *Journal of Physics: Conference Series*, IOP Publishing, vol. 1559, 2020, p. 012 040.

[21] E. H. Brandt, "Superconductors in realistic geometries: Geometric edge barrier versus pinning," *Physica C: Superconductivity*, vol. 332, no. 1-4, pp. 99–107, 2000.

[22] S. Keckert *et al.*, "Critical fields of nb3sn prepared for superconducting cavities," *Superconductor Science and Technology*, vol. 32, no. 7, p. 075 004, 2019.

[23] D. A. Turner, G. Burt, and T. Junginger, "No interface energy barrier and increased surface pinning in low temperature baked niobium," *Scientific reports*, vol. 12, no. 1, pp. 1–9, 2022.

[24] M. Kang, H. N. Han, and C. Kim, "Microstructure and solidification crack susceptibility of al 6014 molten alloy subjected to a spatially oscillated laser beam," *Materials*, vol. 11, no. 4, p. 648, 2018.

[25] Z. Abdulsattar and W. Al-Ashtari, "Effects of laser parameters on solidification cracks formation during lsm treatment for aa6061," *International Journal of Applied Engineering Research*, vol. 13, no. 8, pp. 5614–5617, 2018.

[26] A. Medvid and P. M. Lytvyn, "Dynamic of laser ablation in sic," in *Silicon Carbide and Related Materials 2003*, ser. Materials Science Forum, vol. 457, Trans Tech Publications Ltd, Jun. 2004, pp. 411–414. DOI: 10.4028/www.scientific.net/MSF.457-460.411.

[27] A. Gurevich and G. Ciovati, "Dynamics of vortex penetration, jumpwise instabilities, and nonlinear surface resistance of type-ii superconductors in strong rf fields," *Physical Review B*, vol. 77, no. 10, p. 104 501, 2008.

[28] B. Oripov and S. M. Anlage, "Time-dependent ginzburg-landau treatment of rf magnetic vortices in superconductors: Vortex semiloops in a spatially nonuniform magnetic field," *Physical Review E*, vol. 101, no. 3, p. 033 306, 2020.

[29] O. Malyshev *et al.*, "Final report on thin film technology, aries delivery report d15.4," *Horizon 2020 Research Infrastructures*, 2021.